HHS Public Access

Author manuscript

Nat Commun. Author manuscript; available in PMC 2015 December 25.

Published in final edited form as:

Nat Commun. ; 6: 7458. doi:10.1038/ncomms8458.

Non-redundant Requirement for CXCR3 Signaling during Tumoricidal T Cell Trafficking across Tumor Vascular Checkpoints

ME Mikucki[1], **DT Fisher**[1], **J Matsuzaki**[2], **JJ Skitzki**[1,3], **NB Gaulin**[1], **JB Muhitch**[1], **AW Ku**[1], **JG Frelinger**[5], **K Odunsi**[2,4], **TF Gajewski**[6,7,8], **AD Luster**[9], and **SS Evans**[1,*]

[1]Department of Immunology, Roswell Park Cancer Institute, Buffalo, NY

[2]Center for Immunotherapy, Roswell Park Cancer Institute, Buffalo, NY

[3]Department of Surgical Oncology, Roswell Park Cancer Institute, Buffalo, NY

[4]Department of Gynecologic Oncology, Roswell Park Cancer Institute, Buffalo, NY

[5]Department of Microbiology and Immunology, University of Rochester Medical Center and the Wilmot Cancer Center, Rochester, NY

[6]Department of Medicine, University of Chicago

[7]Department of Pathology, University of Chicago

[8]Comprehensive Cancer Center and Committee on Immunology, University of Chicago

[9]Center for Immunology and Inflammatory Diseases, Division of Rheumatology, Allergy and Immunology, Massachusetts General Hospital, Harvard Medical School, Boston, MA

Abstract

T cell trafficking at vascular sites has emerged as a key step in antitumor immunity. Chemokines are credited with guiding the multistep recruitment of $CD8^+$ T cells across tumor vessels. However, the multiplicity of chemokines within tumors has obscured the contributions of individual chemokine receptor/chemokine pairs to this process. Moreover, recent studies have challenged whether T cells require chemokine receptor signaling at effector sites. Here, we

*Please address all correspondence to Sharon S. Evans, Department of Immunology, Roswell Park Cancer Institute, Buffalo, NY 14263. Phone: (716) 845-3421 Fax: (716) 845-1322 sharon.evans@roswellpark.org.

Author Contributions

M.M. and S.S.E conceptualized and designed the research; S.S.E. supervised the research; M.M. did all experiments unless stated otherwise; D.T.F. performed IVM studies in non-tumor-bearing mice, quantification of T cell extravasation by immunofluorescence microscopy, and together with A.W.K., assisted in therapeutic adoptive transfer experiments and long-term infiltration studies; A.D.L. provided *Cxcr3*$^{-/-}$ OT-I mice and neutralizing CXCL9/CXCL10 Ab as well as contributed to the experimental design and interpretation of the studies; K.O. and J.M. contributed to the intellectual setup and implementation of studies using human PBMC; J.J.S. contributed to experimental design and performed initial studies investigating CXCR3 activity during trafficking; N.B.G and J.B.M helped conceptualize and perform pilot studies identifying intravascular chemokines using fluorescent beads; J.G.F. was involved in experimental design and interpretation of results; T.F.G. provided M537 and M888 melanoma cell lines and participated in research design; and all authors contributed to discussions and preparation of the manuscript.

Competing Financial Interests

The authors declare no competing financial interests.

investigate the hierarchy of chemokine receptor requirements during T cell trafficking to murine and human melanoma. These studies reveal a non-redundant role for $G_{\alpha I}$-coupled CXCR3 in stabilizing intravascular adhesion and extravasation of adoptively transferred $CD8^+$ effectors that is indispensable for therapeutic efficacy. In contrast, functional CCR2 and CCR5 on $CD8^+$ effectors fail to support trafficking despite the presence of intratumoral cognate chemokines. Taken together, these studies identify CXCR3-mediated trafficking at the tumor vascular interface as a critical checkpoint to effective T cell-based cancer immunotherapy.

Introduction

The immune contexture is widely recognized as an important determinant of overall survival in cancer patients[1]. In particular, the presence of cytotoxic $CD8^+$ T cells at high density within tumor tissue is beneficial in multiple cancer types including colorectal, ovarian, and melanoma, and can be a better prognostic indicator of patient outcome than traditional tumor-node-metastasis (TMN) staging[1–6]. Active areas of research seek to improve T cell-mediated immunity in patients by focusing on therapeutics that manipulate either the T cell arm of antitumor immunity or the tumor microenvironment where T cells execute their effector functions[7–9]. The frequency of tumor-specific T cells and their cytotoxic function can be boosted through DC vaccination, adoptive T cell transfer (ACT) therapy, or administration of checkpoint blockade inhibitors (e.g., targeting immunosuppressive molecules such as cytotoxic T-lymphocyte-associated protein 4 [CTLA-4] or programmed-death/programmed-death ligand 1 [PD-1/PD-L1]) and has led to durable responses in a subset of patients[8,10–13]. Alternatively, we and others have converted the tumor microenvironment from relatively ‘low’ to ‘high’ sites of T cell infiltration in preclinical studies using TLR agonists, IFNs, antagonists of endothelin B and angiogenic factors, or interleukin-6 (IL-6)-dependent strategies[9,14–17]. Fundamental to the efficacy of all T cell-based immunotherapy is the requirement for blood-borne T cells to gain entry across tumor vascular gateways in order to engage in contact-dependent lysis of neoplastic targets.

Given the importance of intratumoral localization of T cells for antitumor immunity, there is surprisingly little known about the trafficking cues necessary to direct extravasation of effector T cells across tumor vessels. Chemokines are considered strong candidates for this process based on their well-established role in T cell trafficking to lymphoid organs[18]. In lymph nodes, for example, the interaction between $G_{\alpha i}$-protein-coupled chemokine receptors (e.g., CCR7) on naïve T cells and chemokine (CCL21) displayed on the lumenal surface of blood vessels is an obligate step for triggering LFA-1–dependent stable adhesion and subsequent transendothelial migration[18,19]. Insight into the role of chemokines in the tumor microenvironment stems from correlative studies linking T cell accumulation with multiple chemokine receptors on effector T cells and/or chemokines within the tumor locale[1,20,21]. In this regard, expression of CXCR3 on circulating T cells or its chemokine ligands, CXCL9 and CXCL10, in tumor tissues is associated with elevated intratumoral T cell infiltration and a favorable outcome in melanoma and colorectal cancer patients[1,20–22]. Similar clinical evidence connects CCR5 and its ligands (CCL3, CCL4, and CCL5), as well as CCR2 and its ligand CCL2, to intratumoral T cell infiltration and disease-free survival[1,20,21]. These observations are suggestive of redundant functions by chemokine receptors during T cell

homing into tumors although chemokines could alternatively orchestrate T cell activities within the tumor interstitium (e.g., proliferation, survival, retention, or egress)[19]. Moreover, the prototypical role for chemokines has recently been challenged by reports in non-tumorigenic inflammatory settings that $CD8^+$ effector T cells with high LFA-1 expression bypass chemokine requirements for stable adhesion within vessels[23,24]. Thus, in the absence of a head-to-head comparison of the chemokine receptor usage at the tumor vascular interface, it remains unclear whether chemokines are operative during T cell entry into tumors or if there is any preferential role for individual chemokine receptors/chemokine pairs during extravasation.

Here, we investigated the hierarchy of chemokine receptor requirements during T cell trafficking by tracking the fate of adoptively transferred $CD8^+$ effector T cells in murine and human melanoma tumors. We compared the functions of three chemokine receptors previously implicated in intratumoral $CD8^+$ effector T cell infiltration (i.e., CXCR3, CCR5, and CCR2) in tumors expressing complementary chemokine ligands. These studies unexpectedly reveal a non-redundant requirement for the CXCR3-CXCL9/CXCL10 axis for $CD8^+$ T cell trafficking within the intravascular space that could not be predicted from static profiling of intratumoral chemokines or their receptors on T cells. We further establish a causal link between CXCR3-dependent trafficking and the efficacy of adoptive T cell transfer therapy. These findings identify CXCR3 interactions with cognate chemokines within the vessel wall as a critical checkpoint dictating the efficacy of T cell-based cancer immunotherapy.

Results

Tumor microenvironment enriched for T cell chemoattractants

To address the chemokine receptor requirements during T cell homing, we first characterized the chemokine milieu in highly aggressive, orthotopic B16 murine melanoma expressing the surrogate tumor antigen ovalbumin (OVA)[14]. For these studies, we focused on inflammatory chemokines previously implicated in T cell infiltration in patient tumors[1,3,9,20]. High concentrations (~1 ng per mg total protein) of CXCL9, CXCL10 (i.e., the two CXCR3 ligands expressed in the C57BL/6 strain[25]), CCL5 (CCR5 ligand), and CCL2 (CCR2 ligand) were detected in B16-OVA tumor extracts compared to non-inflamed normal skin following subcutaneous injection of PBS (Fig. 1a).

Complementary studies profiled $CD8^+$ effector T cells for functional receptors specific for the inflammatory chemokines found in the tumor microenvironment. Chemotactic activity was tested in vitro for $CD8^+$ T cells from OVA-specific OT-I transgenic mice [wild-type (WT)] or chemokine receptor-deficient mice that were activated ex vivo to simulate the expansion of T cells for clinical ACT immunotherapy[12,14,26]. WT OT-I effector populations (>96% $CD8^+CD44^{hi}$, Supplementary Fig. 1a) exhibited strong migration to recombinant CXCL9, CXCL10, CCL5, and CCL2, that was blocked by pertussis toxin (PTX), a global inhibitor of $G_{\alpha i}$ protein-coupled chemokine receptor signaling (Fig. 1b). Genetic deletion of *Cxcr3* (crossed on an OT-I background; *Cxcr3*$^{-/-}$ OT-I) or *Ccr5* and *Ccr2* (on a C57BL/6 background) was further shown to specifically block T cell migration to its cognate ligands without impairing the response to other ligands (Fig. 1b). $CD8^+$ $CD44^{hi}$ T cells activated ex

vivo exhibited a CXCR3^{hi} CCR2$^{int/lo}$ CCR5$^{int/lo}$ phenotype which was also typical of CD8^{+} T cells activated in vivo (i.e., detected in draining nodes following DC vaccination or tumor implantation; Supplementary Fig. 1b). Collectively, these data indicate that CD8^{+} effector T cells express a repertoire of functional chemokine receptors which would be expected to guide trafficking to chemokine-rich tumors in situ.

CXCR3 signaling obligate for intratumoral T cell trafficking

Short-term (1 hour) competitive homing assays were used[14,27] to determine whether $G_{\alpha i}$-chemokine signaling was obligatory for T cell trafficking in B16-OVA. In these assays, WT effector OT-I cells were admixed at a 1:1 ratio with PTX-pretreated WT OT-I T cells (labeled with different tracking dyes) prior to intravenous ACT (Fig. 2a). After 1 hour, the ratio of T cells was determined in tumor tissues by flow cytometry, and data are reported for homing relative to untreated WT OT-I cells. This 1 hour time-frame enabled us to discriminate chemokine functions specifically at the vessel wall since it is sufficient for cells to complete steps leading to extravasation[14], but not long enough for other processes to occur that influence the extent of T cell infiltration (i.e., proliferation in situ, survival, retention and egress). Homing of PTX-treated OT-I was less efficient than WT OT-I, as indicated by the 1:3 ratio of PTX:WT cells recovered in tumors (Fig. 2b). This was in contrast to control experiments where a 1:1 ratio of intratumoral WT:WT cells was detected. Access of effector T cells to the spleen via the peripheral circulation was not affected by functional chemokine receptor status (Fig. 2b). These data establish that $G_{\alpha i}$-coupled chemokine receptor signaling is necessary for effector CD8^{+} T cell homing in tumors.

We next investigated whether there was a hierarchy of chemokine receptor usage during extravasation into tumor tissue. Initial studies focused on CXCR3 requirements for the entry of adoptively transferred effector T cells in competitive (1 hour) homing assays in which WT OT-I cells were admixed with *Cxcr3*$^{-/-}$ OT-I T cells or with OT-I cells pre-treated with a CXCR3-blocking antibody (Ab). Surprisingly, despite expression of functional CCR5 and CCR2 (Fig. 1b), loss of the single chemokine receptor, CXCR3, reduced T cell trafficking to the same extent as global blockade of chemokine signaling by PTX (Fig. 2b). Further head-to-head comparison of admixed PTX-pretreated and *Cxcr3*$^{-/-}$ OT-I cells in the same recipient mice substantiated that CXCR3 accounted for all $G_{\alpha i}$-coupled chemokine receptor-dependent trafficking by CD8^{+} effectors in B16-OVA melanoma (Supplementary Fig. 2a). Microscopic quantification of homed cells within the interstitium (i.e., T cells located outside CD31^{+} vessels in tumor sections) further demonstrated an absolute requirement for CXCR3 during T cell extravasation (Fig. 2c). Contributions of other chemokine receptors failed to emerge even when the overall rate of trafficking was improved (~2 fold) using an IL-6–dependent thermal preconditioning strategy (core body temperature elevated to 39.5 ± 0.5°C, 6 h) that targets the tumor vasculature to be more permissive for T cell homing[14] (Fig. 2d and Supplementary Fig. 2b). CXCR3 dependency was also evident during endogenous CD8^{+} T cell infiltration in tumors implanted in WT mice and *Cxcr3*-deficient mice (Supplementary Fig. 2c), suggesting that the same CXCR3 bias exists whether T cells are activated ex vivo or in vivo. Collectively, these data establish a non-redundant role for CXCR3-mediated $G_{\alpha i}$ protein signaling during emigration of blood-borne CD8^{+} effector T cells in the tumor microenvironment.

CXCR3 ligands mediate T cell firm arrest in tumor vessels

Our findings demonstrated that CXCR3 is required at some point during the multistep migration process leading to $CD8^+$ effector T cell migration. These observations prompted our use of epifluorescence intravital microscopy to examine whether CXCR3 plays a prototypical role in triggering T cell adhesion[18,19] within the intravascular space in tumor tissues. Since our prior studies established that the frequency of baseline adhesive interactions between effector T cell and tumor vessels is near the lower limit of detection by live imaging[14], we administered thermal therapy to augment homing in order to interrogate subtle chemokine requirements. PTX-uncoupling of $G_{\alpha i}$ protein signaling or genetic deletion of *Cxcr3* had no impact on the ability of OT-I cells to initiate rolling interactions within tumor vessels but strongly inhibited the transition to firm arrest (Fig. 3a). Notably, WT and *Cxcr3*$^{-/-}$ effector OT-I expressed comparable levels of adhesion molecules necessary for rolling and firm arrest (i.e., E/P-selectin ligands and CD11a [the α subunit of LFA-1], respectively; Supplementary Fig. 3a). The dependence on $G_{\alpha i}$ protein signaling further was not unique to tumor vessels since PTX-pretreated OT-I effectors exhibited significantly reduced firm arrest of $CD8^+$ effectors in inflamed skin vessels of non-tumor-bearing mice stimulated with the TLR4 agonist, LPS (Supplementary Fig. 3b).

To determine if there was a preferential contribution for individual CXCR3 ligands for trafficking, we adapted an approach described previously to visualize membrane-anchored adhesion molecules in lymph node vasculature[28] in order to determine which CXCR3 ligands were available in the intravascular space. In the present study, intravascular chemokines were quantified microscopically in tissue sections following intravenous injection of fluorescent beads conjugated with CXCR3 ligand-specific Ab. These studies focused on CXCL9 and CXCL10 since C57BL/6 mice do not express CXCL11[25,29]. Both CXCL9 and CXCL10 were displayed within tumor vessel walls as indicated by specific accumulation of α-CXCL10 and α-CXCL9 Ab-conjugated beads in $CD31^+$ vessels compared to isotype controls (Fig. 3b), whereas CXCR3 ligand-conjugated beads were not evident in normal tissues (e.g., pancreas). We then employed a chemokine blocking strategy in which tumor-bearing mice were pre-treated with blocking Ab to CXCL9, CXCL10, or combined CXCL9/CXCL10[25,30] prior to adoptive transfer of admixed WT:*Cxcr3*$^{-/-}$ T cells (Fig. 3c). Partial inhibition of $CD8^+$ T cell homing was observed with single chemokine blockade whereas complete inhibition occurred upon dual targeting of CXCL9 and CXCL10 (i.e., as indicated by 1:1 ratio of WT:*Cxcr3*$^{-/-}$ cells recovered at tumor sites following dual Ab blockade which was equivalent to the input ratio; Fig. 3c). There was no change in the spleen, confirming that the inhibitory effects on intratumoral homing cannot be attributed to Ab-mediated T cell clearance. Taken together, these data identify CXCR3 interactions with intravascular ligands as a critical step leading to stable adhesion and subsequent transendothelial migration of adoptively transferred $CD8^+$ effector T cells at tumor sites.

CCR5 and CCR2 are dispensable for T cell homing to tumors

Results that CCR5 and CCR2 were unable to compensate for loss of CXCR3 in vivo do not exclude the possibility that these chemokine receptors cooperate with CXCR3 to control adhesion in tumor vessels. There is already precedent for cooperativity involving these chemokine receptors[31,32]. For example, physical interactions between CCR5 and CXCR4

are required for CXCR4-mediated enhancement of T cell activation in vitro [32] while simultaneous exposure of cells to CCL2 and CCL5 lowers the threshold for downstream calcium mobilization[31].

To assess whether CCR5 or CCR2 were operative in the context of CXCR3-dependent T cell trafficking, we first established that CCL5 and CCL2 were also available in the tumor intravascular space, as would be necessary to coordinate with CXCR3 ligands during extravasation (Fig. 4a). We then performed competitive homing studies to examine the ability of *Cxcr3*$^{-/-}$, *Ccr5*$^{-/-}$, or *Ccr2*$^{-/-}$ CD8^{+} effector CD8^{+} T cells to traffic compared to WT (Fig. 4b). In these experiments the T cells used to track homing were from normal C57BL/6 mice, not the OT-I background. Consistent with our results for OT-I cells, trafficking was markedly inhibited by PTX-treatment of WT cells or *Cxcr3* deficiency, indicating that recognition of cognate tumor-associated antigen is not necessary for CXCR3-dependent T cell extravasation at tumor loci. Conversely, loss of *Ccr2* or *Ccr5* did not compromise T cell entry into B16-OVA tumors or in peripheral sites such as the spleen (Fig. 4b). Of note, while CCR2 did not contribute to T cell trafficking, there was sufficient ligand available to support CCR2-dependent intratumoral recruitment of CD115^{+} inflammatory monocytes[33] that have high CCR2 expression relative to CD8^{+} effectors (Fig. 4c and 4d; Supplementary Fig. 4). Since CCL2 and CCL5 have been implicated in T cell diapedesis in vitro[23], we also considered whether *Ccr5*$^{-/-}$ and *Ccr2*$^{-/-}$ T cells were defective in their ability to migrate through tumor vessel walls which would not be discernible by flow cytometric analysis. Microscopic analysis did not reveal a disproportionate accumulation of adoptively transferred *Ccr5*$^{-/-}$ or *Ccr2*$^{-/-}$ T cells within tumor vessels nor a concomitant defect in extravasation (Fig. 4e). Overall, these data demonstrate that CCR5 and CCR2 are not required to cooperate with CXCR3 during T cell extravasation across tumor vessels.

Efficacy of adoptive transfer cell therapy depends on CXCR3

Evidence that CXCR3 directs homing of adoptively transferred CD8^{+} T cells at the tumor vascular interface prompted us to investigate the relationship between CXCR3 and antitumor immunity. In these studies we initially characterized the cytotoxic activity of WT and *Cxcr3*$^{-/-}$ OT-I T cells in assays where effectors have ready access to cognate targets. Activated *Cxcr3*$^{-/-}$ and WT OT-I cells were indistinguishable with respect to IFN-γ and granzyme B expression (Supplementary Fig. 5a) and exhibit equivalent specific cytotoxicity against cognate targets in vitro including splenocytes pulsed with SIINFEKL OVA peptide, B16-OVA, or OVA-expressing EG7 lymphoma (Supplementary Fig. 5b–d). Parallel results were obtained during in vivo cytotoxicity assays against SIINFEKL-pulsed splenocyte targets within the splenic compartment (Fig. 5a). These findings are in line with evidence that CXCR3 deficiency does not compromise localization of adoptively transferred CD8^{+} T cells within the spleen (Fig. 2b).

To test the cytotoxic activity of T cells in tumors where entry depends on CXCR3, we adoptively transferred a single dose of WT or *Cxcr3*$^{-/-}$ OT-I effector T cells intravenously into mice and monitored B16-OVA tumor progression. These studies exploited the OT-I TcR transgenic model system in order to dissect the therapeutic impact of chemokine-dependent trafficking without masking chemokine contributions due to weak TCR affinity/

avidity for tumor antigen. WT OT-I T cells caused a significant delay in tumor growth and prolonged survival, with cures detected in some experiments (Fig. 5b, Supplementary Fig. 6a). Conversely, $CD8^+$ effectors lacking *Cxcr3* provided no therapeutic benefit, compared to untreated controls, in this stringent model where 100% of transferred cells were tumor (OVA)-reactive. Kinetic studies performed after adoptive transfer showed a progressive increase in the extent of intratumoral infiltration by WT OT-I cells, but not *Cxcr3*$^{-/-}$ OT-I (monitored using tracking dye or CD45 congenic mismatch), underscoring the CXCR3 requirements for tumor immunity (Fig. 5c, Supplementary Fig. 6b). Additionally, we found that a high intratumoral density of WT OT-I (~10,000 OT-I per 10^6 total cells within tumors) correlated directly with tumor control in the majority of mice analyzed at 3 weeks post-adoptive transfer (i.e., tumors < 20 mm^3 in 9/12 mice) (Fig. 5d). Conversely, WT OT-I were present at a low density (~50 OT-I/10^6 total cells in tumors) in the subgroup of mice in which tumors were progressing (tumors >450 mm^3 in 3/12 mice). Notably, the tumor volume and density of WT OT-I cells detected in progressing tumors was indistinguishable from observations in 100% of mice treated with *Cxcr3*$^{-/-}$ OT-I that failed to reject tumors (Fig. 5d). These results are consistent with a prior report showing that OT-I must exceed a critical threshold within B16-OVA tumors for ACT immunotherapy to be successful[34]. Collectively, these data indicate that CXCR3-dependent signaling at the tumor vascular barrier is a critical checkpoint for the efficacy of adoptively transferred T cells.

Human effector T cells require CXCR3 for homing in melanoma

In light of the importance of CXCR3-dependent trafficking for antitumor immunity following adoptive T cell transfer therapy in mice, we extended our analysis of chemokine requirements to the trafficking of human effector T cells to human melanoma xenografts comprised of the M537 and M888 patient-derived melanoma cell lines[20,35,36]. We initially profiled chemokine receptor expression by human T cells that were activated and expanded ex vivo using clinical ACT protocols for cancer patients[12,26,37]. Activated PBL populations from normal donors (n=7) were predominantly $CD3^+$ (>97%) with robust CXCR3 expression on $CD8^+$ cells (i.e., the major T cell subset), while CCR2 and CCR5 were highly variable among individual donors as reported previously[20,37,38] (Fig. 6a, Supplementary Fig. 7a). Chemotaxis assays in vitro further validated that activated human T cells expressed functional CXCR3, CCR5, and CCR2 which responded to both human and murine chemokines (Supplementary Fig. 7b). Since our studies with murine $CD8^+$ effector T cells raised the possibility that limited CCR2 or CCR5 expression might be responsible for the failure to detect CCR2- or CCR5-dependent trafficking to murine melanoma, we selected representative donor T cell populations for adoptive transfer experiments that dually expressed high CXCR3/CCR2 (donor 1) or high CXCR3/CCR5 (donor 2) (Fig. 6a).

To survey the chemokine milieu available to adoptively transferred T cells in human melanoma xenografts, we measured both tumor-derived (human) and stromal-derived (murine) chemokines produced in the local tumor milieu. Differential production of tumor-derived (human) CXCL9, CXCL10, CXCL11, CCL2, and CCL5 was observed in M537 and M888 xenografts in vivo (Fig. 6b) which is largely in line with previous in vitro observations[20]. However, stromal-derived murine chemokines represented the vast majority of local chemokine and were detected at similar levels in M537 and M888 tumor extracts

(Fig. 6b). Thus, M537 and M888 tumors had similar chemokine microenvironments when considering the combined contributions from both mouse and human chemokines, allowing for chemokine-dependent trafficking to be investigated in both tumor systems.

Short-term competitive homing assays were then used to examine CXCR3 contributions during human T cell trafficking to melanoma xenografts (Fig. 6c). CXCR3 activity was specifically disrupted on activated PBL prior to adoptive transfer with a blocking Ab that reportedly inhibits CXCR3-mediated migration in vitro[39]. As a second method, we desensitized T cells with recombinant CXCL10 to downregulate surface expression of CXCR3[40]. CXCR3 inactivation by these approaches was confirmed by flow cytometry or in vitro chemotaxis assays (Supplementary Fig. 7c). Data in Fig. 6c demonstrate that loss of CXCR3 activity by Ab blockade or desensitization diminished homing of T cells from both donor 1 and donor 2 in M537 and M888 melanoma xenografts to the same extent as PTX-pretreatment but did not alter localization in the spleen (Fig. 6c, Supplementary Fig. 8a). Homed cell populations in tumors were ≥65% $CD8^+$ T cells, which were reflective of the predominantly $CD8^+$ T cell input population (Fig. 6a). Thus, high expression of CCR2 or CCR5 by human effector T cells could not compensate for the absence of CXCR3. The CXCR3 requirement for trafficking in M537 and M888 was further validated in competitive homing assays using murine WT and *Cxcr3*$^{-/-}$ $CD8^+$ effector T cells (Supplementary Fig. 9a,b). Taken together, these data unequivocally show a non-redundant role for CXCR3 in trafficking of $CD8^+$ human effector T cells in melanoma during adoptive T cell transfer immunotherapy.

Discussion

Successful delivery of blood-borne $CD8^+$ effector T cells across the tumor vasculature is recognized as a key determinant of antitumor immunity. However, to date, there is no information about the hierarchy of chemokine receptors that guide tumoricidal T cells into the tumor microenvironment. Here, we report on the non-redundant function of CXCR3 and its complementary intravascular ligands during $CD8^+$ T cell trafficking to tumor tissues. The requirement for CXCR3 is shared by both murine and human $CD8^+$ effector T cells and is necessary for the efficacy of adoptive T cell transfer therapy in the B16-OVA tumor model. These findings provide mechanistic insight for observations in cancer patients that CXCR3 expression by circulating T cells and intratumoral CXCR3 ligands are independent indicators of a favorable prognosis[21,22]. Surprisingly, CCR5 and CCR2 did not contribute to T cell trafficking across tumor vessels despite the presence of cognate chemokines in the tumor microenvironment. These findings highlight the disconnect between functional readouts from in vitro chemotaxis assays and in vivo trafficking. Our results corroborate observations that the chemotactic response to soluble chemokine does not reflect the pro-adhesive signals delivered by immobilized chemokine on two dimensional endothelial surfaces[41–43]. Collectively, these studies reveal a unique role for CXCR3/CXCR3 ligands in cancer immunotherapy in vivo that could not be predicted from genomic and proteomic profiling of the inflammatory signature in the tumor microenvironment.

Our findings, together with recent reports[23,24], suggest that the dependence of effector T cells on $G_{\alpha i}$ protein signaling at the vascular interface is dictated by the inflammatory

context, thus having broad implications outside the tumor milieu. Central to these studies was the discrimination of $G_{\alpha i}$-dependent trafficking mechanisms using PTX which irreversibly uncouples $G_{\alpha i}$ protein signaling from chemokine receptor/ligand binding[19]. Our data establish the requirement for PTX-dependent signaling during the transition of $CD8^+$ effector cells from rolling to firm arrest in tumor vessels as well as in normal vessels in the context of LPS-induced systemic inflammation. This requirement is in line with evidence that CXCR3 contributes to $CD8^+$ T cell localization in inflamed normal skin[19,44,45] as well as the prevailing view whereby chemokines trigger a conformational change in LFA-1, resulting in an ~500-fold increased affinity for ICAM-1 that stabilizes intravascular adhesion[19,46]. Intermediate chemokine receptor requirements were described during DTH responses in which $CD8^+$ effectors bypass $G_{\alpha i}$ protein signaling during the firm adhesion step, and instead rely primarily on CCR2 during transendothelial migration[23]. Cardiac allograft rejection models represent the other end of the spectrum where extravasation of $CD8^+$ effector T cells is completely independent of $G_{\alpha i}$ protein signaling[24]. The reasons for these differential chemokine requirements are unclear, but likely involve variability within the tissue microenvironment rather than T cell behavior since each of these disparate reports used activated OT-I $CD8^+$ effector T cells. One possibility is that differences in downstream TLR signaling following induction of local DTH by injection of complete freund's adjuvant[23] (via TLR2[47]) or by systemic LPS administration (via TLR4[48]) account for distinct chemokine receptor requirements in the intravascular space[49]. A key difference between the allograft model and our studies is that $G_{\alpha i}$-independent trafficking occurs as a consequence of TcR activation by transplant antigens presented by vascular endothelium or nearby DCs[24]. In contrast, results of the current study combined with our previous findings[14] indicate that trafficking of murine T cells or normal donor-derived human $CD8^+$ effectors to tumors or inflamed tissues is not antigen-restricted, which may serve to reinforce T cell dependence on intravascular chemokines.

Observations that CCR2 and CCR5 do not participate during $CD8^+$ effector T cell trafficking into melanoma tumors raise questions about how CCR2 supports monocyte homing in the same intravascular chemokine environment. This could be explained, in part, by the recently discovered post-translational nitration of CCL2 which supports monocyte but not effector T cell chemotaxis in vitro[38]. Nitrated CCL2 is found in the tumor microenvironment of murine and human colon and pancreatic tumors[38], presumably modified by nitric oxygen species derived from local protumorigenic myeloid cells. Furthermore, global blockade of peroxynitrite enhances T cell infiltration and decreases detectable nitrated CCL2 in murine tumors, although a cause-and-effect relationship for these observations remains to be established[38]. The commercial Ab used to detect intravascular CCL2 in our studies does not appear to recognize nitrated CCL2 in tumor tissues[38] (Dr. Barbara Molon, personal communication), so there may still be a substantial pool of nitrated CCL2 on the intravascular surface which could preferentially support monocyte trafficking. Differential migratory responses of monocytes and T cells to nitrated CCL2 in vitro have been attributed to higher CCR2 surface expression on monocytes[38], a distinction that we also observed for murine $CD115^+$ inflammatory monocytes and $CD8^+$ effectors.

Evidence that human effector $CD8^+$ T cells expressing high levels of CCR2 or CCR5 failed to utilize these receptors during trafficking to human melanoma tumors suggests that deficient receptor expression cannot fully account for the selective dependence of $CD8^+$ effectors on CXCR3 in vivo. These results indicate that there may be cell-intrinsic properties that impact chemokine receptor activity in vivo, such as variations in the availability of molecules which regulate $G_{\alpha i}$ protein signaling downstream of receptor activation. Strong candidates for cell-specific negative regulation include G protein-coupled receptor kinases (GRK), which phosphorylate the C-terminal intracellular loop of chemokine receptors to prevent the association of heterotrimeric $G_{\alpha\beta\gamma}$ complexes[50,51], and regulators of G protein signaling (RGS), which accelerate the exchange of GTP on active G_{α} subunits to limit signal duration[50–52]. Notably, the GRK2 isoform is elevated in activated human T cells compared to monocytes[53,54] and is implicated in repressing both CCR2 and CCR5 signaling[55,56]. Similarly, elevated expression of RGS-1 has been reported in activated T cells compared to peritoneal macrophages[57]. Thus, it is likely that the net balance of regulatory molecules for $G_{\alpha i}$ signaling within cells has a substantial impact on the ability of $CD8^+$ effectors to respond to intravascular CCR2 and CCR5 ligands in tumors.

Our data support a scenario whereby CXCR3-dependent delivery of blood-borne T cells at the vascular juncture is a critical step in therapeutic antitumor immunity. Since CXCR3, CCR5, and CCR2 are all associated with overall levels of T cell infiltration and positive outcomes in cancer patients[1,20,21], it is tempting to speculate that signaling through these or other $G_{\alpha i}$-linked receptors support the antitumor activity of $CD8^+$ T cells within the interstitium via mechanisms independent of extravasation. For example, in vitro studies have shown that CXCR3 and CCR5 enhance T cell activation and proliferation[58,59] while CCL2 can increase the cytotoxicity of T cells engineered to co-express CCR2 and chimeric antigen receptors[60]. Additionally, ligand engagement of the $G_{\alpha i}$-coupled leukotriene B4 (LTB4) receptor (BLT) has been linked to increased accumulation of $CD8^+$ T cells and T cell-mediated antitumor immunity in murine cervical cancer model[61]. Although not addressed in the current study, CXCR3 on T cells could also function outside tumor tissues by regulating antitumor immunity within lymphoid organs. In this regard, CXCR3 has already been implicated in non-tumor systems in guiding $CD4^+$ or $CD8^+$ T cell positioning near antigen-loaded DCs within lymph nodes and the spleen during T cell priming and the generation of effector populations[25,62]. These observations are highly relevant to preclinical and clinical adoptive T cell transfer therapy in which the efficacy depends on direct cytotoxic functions of effector T cells within tumors as well as seeding of lymphoid organs by memory T cells to perpetuate long-term antitumor immunity[8,12,14,18].

In summary, this report identifies the interface between CXCR3 on effector T cells and chemokine ligands within tumor vessels as a critical checkpoint dictating the efficacy of T cell-based cancer immunotherapy. The experimental strategy used here to interrogate the homing properties of large numbers of transferred T cells is analogous to clinical adoptive transfer protocols where the goal is to massively expand the tumor-specific T cell pool. As an example, recent studies have shown that it is technically feasible to transfer > 120 billion tumor-reactive T cells in a patient in a bolus injection[63]. Given our observations that CXCR3 is also required for intratumoral localization of endogenous $CD8^+$ T cells, it is likely that conclusions regarding biased CXCR3 usage are also relevant to other

immunotherapies in which a lower frequency of tumor-reactive T cells might be generated. Similar CXCR3 requirements for homing of $CD8^+$ effectors may also be operative in other orthotopic murine tumors such as the PyMT breast tumor model, which exhibits more aggressive growth after implantation in *Cxcr3*$^{-/-}$ hosts because of M2 macrophage polarization[64].

These observations provide guidance for which chemokine receptor/chemokine pair could be exploited clinically to improve antitumor immunity. Our results, together with other published studies, demonstrate that there is universally high CXCR3 expression on ex vivo activated human T cells either from normal donors or cancer patients[20,37]. Thus, inadequate expression of CXCR3 does not appear to be an obstacle to adoptive T cell immunotherapy. In contrast, the tumor microenvironment is highly variable with respect to CXCR3 ligand expression[1,20,21,37]. This raises the possibility of using therapeutic strategies to boost CXCR3 ligands in the tumor locale which could be shuttled out onto the endothelial surface through the process of transcytosis[65,66]. Several approaches being studied clinically to promote an antitumorigenic inflammatory gene signature such as administration of TLR ligands (e.g., CpG or poly I:C), or IFN-α have been shown in preclinical studies to induce production of CXCR3 ligands by intratumoral stromal cells (fibroblasts, monocytes, or $CD45^+$ leukocytes)[9,15,67]. Commonly used chemotherapeutic agents such as cisplatin and temozolomide similarly boost tumor cell expression of CXCR3 ligands in preclinical melanoma models, paralleling the increases in CXCL9 and CXCL10 gene expression detected in melanoma patient tumors after treatment with dacarbazine[68]. Moreover, intratumoral injection of recombinant CXCL10 or adenovirus encoding CXCL10 reportedly contributes to $CD8^+$ T cell infiltration and tumor rejection in murine tumors[69,70]. Based on our current findings, we would predict that chemokine-targeting strategies further offers promise in an adjuvant setting with adoptive T cell transfer therapy, cancer vaccines, or checkpoint blockade inhibitors that rescue $CD8^+$ T cell function by disrupting CTLA-4 and PD-1/PD-L1-mediated immune-suppressive networks[8,10,11,13]. It is noteworthy, in this regard, that elevated *CXCL9* expression in patient melanoma specimens correlates with response to PD-L1 blockade therapy[13].

Methods

Animals

Female age-matched C57BL/6 and OT-I mice on a CD45.1 background (B6.129S7-Rag1tm1Mom Tg[TcraTcrb]1100Mjb) (8–12 weeks) were from the National Cancer Institute or Taconic; C57BL/6 with CD45.2 phenotype (B6.SJL-Ptprca Pepcb/BoyJ), C*cr5*$^{-/-}$ *(*B6.129P2-Ccr5tm1Kuz/J), and *Ccr2*$^{-/-}$ *mice (*B6.129S4-Ccr2tm1Ifc/J) were from Jackson Laboratory and bred in-house along with C*xcr3*$^{-/-}$ OT-I (on a C57BL/6/CD45.1 background as described [29]) and SCID mice (SCID C.B Igh-1b Icr Tac Prkdc scid) in the Roswell Park Department of Laboratory Animal Resources. Animal protocols were approved by the Roswell Park Cancer Institute Institutional Animal Care and Use Committee.

Tumor models

B16-OVA cells and parental B16 were cultured in complete media (RPMI 1640 supplemented with 10% FCS, 2 mM L-glutamine, 100 U/ml penicillin, 50 μg/ml streptomycin, and 50 μM β-mercaptoethanol [Invitrogen]). M537 and M888 cells were cultured in complete media lacking β-mercaptoethanol[20,35,36]. EL4 and EG7 cells were cultured in complete media supplemented with 1 mM sodium pyruvate, MEM non-essential amino acids, 25 mM HEPES (Invitrogen); media for EG7 cells contained 40 μg/mL G418 sulfate (LifeTechnologies). Tumor cells (10^6) were injected subcutaneously in the flank of C57BL/6 mice or SCID mice as previously described[14,20] and used for experimental analysis when tumor volume reached ~400–500 mm^3 (~10–14 days or 6–8 weeks post-implantation for murine and human melanoma, respectively) unless otherwise indicated.

T cell activation ex vivo or in vivo

Pooled murine splenocyte/lymph node populations (2×10^6 cells/ml) were activated for 2 days in 24-well plates (Corning) coated with anti-mouse CD3 Ab (2.5 μg/ml; Cat # 550275 clone 145–2C11; BD Biosciences) in complete media (including MEM non-essential amino acids, 20 mM HEPES, 1.5 mM sodium pyruvate); then diluted to 2×10^5 cells/ml, and expanded for 3 days with recombinant human IL-2 (12.5 ng/ml; Peprotech). Human PBMC were isolated from anonymous normal donor buffy-coats obtained from the Roswell Park blood donor center by centrifugation on a Ficoll–Hypaque gradient, washed with HBSS, and suspended in complete media (with 100 μg/ml streptomycin and without β-mercaptoethanol). PBMC were activated for 2 days with anti-human CD3 Ab (2 μg/ml; Cat# 16-0037-81 OKT3; eBiosciences) and anti-CD28 Ab, then expanded for 5 days with recombinant human IL-2 (300 IU/ml; Novartis). All Ab and cytokines were azide and endotoxin-free. DC vaccination was performed to activate $CD8^+$ $CD44^+$ T cells in vivo. Mouse bone marrow-derived DCs were generated by culturing bone marrow cells for 8 days in media used for murine T cell activation, supplemented with murine GM-CSF (~20 ng/ml; provided by Dr. Kelvin Lee, Roswell Park Cancer Institute). DCs were matured by LPS treatment (0.5 μg/ml) overnight, then pulsed with 5 μM SIINFEKL peptide (InvivoGen), and 3×10^6 DCs were injected into the hind footpad; T cells were recovered from draining nodes (popliteal, inguinal) after 7 days. As an alternative method for in vivo activation, T cells were analyzed in draining nodes (inguinal) 7 days after B16-OVA tumor implantation.

Treatment with STT, LPS, or cytokine-neutralizing reagents

Mice were treated with systemic thermal therapy (STT; core temperature of 39.5 ± 0.5°C, 6 h) and allowed to return to baseline temperature prior to homing studies as described[14,27]. LPS (1 mg/kg; Sigma) was injected i.p. 6 h prior to trafficking studies[14]. Neutralizing polyclonal anti-CXCL9 or anti-CXCL10 Ab[30] (100 μg/mouse) or polyclonal isotype IgG control (cat# BE0091 100 μg/ mouse; BioXCell) were injected i.p. 3 h prior to competitive homing studies. Murine activated $CD8^+$ T cells were pretreated with pertussis toxin (100 ng/ml, 2.5 h; Sigma), or anti-mouse CXCR3 blocking Ab (cat# 126526 100 μg/mL, 1h; Biolegend). Human activated T cells were pretreated with pertussis toxin, human CXCR3 functional blocking Ab (cat# LS-C6283-500 40 μg/ml, 30 min; LifeSpan BioSciences, Inc[39]), or human recombinant CXCL10 (500nM, 30 m; Peprotech) to desensitize CXCR3[40].

Quantification of tissue and intravascular chemokines

Soluble extracts from tumor or normal skin were prepared by dissociating tissue by Medimachine (BD Biosciences) in the presence of protease inhibitors (CalBiochem). Chemokines were measured by ELISA (R&D Systems and Antigenix) or Luminex (Procarta) and normalized to total protein concentrations determined by Bradford analysis (Bio-Rad)[14]. Normal skin samples were from mice that received a s.c. injection of 100 μl sterile PBS 12 day prior to tissue harvest to mimic any needle-derived inflammation at the injection site. Intravascular chemokines were detected by adapting methodology used to identify intravascular adhesion molecules in LN[28]. Briefly, yellow-green fluorescent sulfate microspheres (Ex/Em 505/515, 1.0 μm diameter, Life Technologies) were labeled with 10 μg/mL of Ab specific for mouse chemokines including anti-CXCL10 (cat# MAB466-500 clone 134013), anti-CXCL9 (cat# AF392 affinity-purified polyclonal Ab), anti-CCL5 (cat# MAB478 clone 53405), anti-CCL2 (cat# BAF479 biotinylated affinity purified polyclonal goat Ab), or isotype-matched control Abs (R&D Systems)[28] and injected i.v. into tumor-bearing mice. After 1 h, tumor and pancreas were frozen in OCT (Sakura Finetek), and then counterstained using anti-mouse CD31 Ab (cat# 550274 clone MEC 13.3, 20 μg/ml; BD Biosciences) followed by an AMCA fluorochrome-conjugated goat anti-rat secondary Ab (cat# 112-155-003 1:50 Jackson ImmunoResearch). For consistency, fields containing a minimum of 1 fluorescent bead were imaged by observers blinded to sample identity, and the number of fluorescently beads associated with $CD31^+$ vessels was quantified in ≥10 fields (unit area per field, 0.34 mm^2) using Image J software (http://rsb.info.nih.gov/ij) as described[14].

Flow cytometry

Multiparameter flow cytometric analysis of murine immune cell phenotype was performed by staining with the following mAb: anti-CD44 (Cat# 561859 clone IM7, FITC, 1:50), anti-CD11a (cat# 553120/cat# 558191 clone 2D7, FITC/PE, 1:100), anti-CD8a (cat# 553036 clone 53–6.7, PerCP, 1:100; cat# 552877 clone 53-6.7, Pe-Cy7, 1:500), anti-CD11b (cat# 561098 clone 1M/70, PE-Cy7 1:100), anti-Ly6C (cat# 560595 clone AL-21, APC, 1:100), anti-CCR5 (cat# 559923 clone C34-3448, PE, 1:20), anti-CD45.1 (cat# 560578 clone A20, PE-Cy7, 1:100), anti-CD45.2 (cat# 560695 clone 104, PE, 1:100), and CD3 (cat# 555274 clone 17A2, FITC, 1:100) (BD Biosciences); anti-CXCR3 (cat# FAB1685A clone 220803, APC, 1:5), anti-CCR2 (cat# FAB5538A clone 475301, 1:5) (R&D Systems); anti-granzyme B (cat# 50-8898, eFluor660, 1:100), anti-IFN-γ (cat# 17-7311-82 clone XMG1.2, APC, 1:100) (eBioscience); and anti-CD115 (cat# 130-102-554 clone AFS98, PE, 1:20; Miltenyi). Functional P-selectin and E-selectin ligands were detected with CD62P or CD62E-IgG fusion proteins, respectively (cat# 737-PS/575-ES, 1:50, R&D Systems). Human T cells were stained with the following Ab: Zombie UV Fixable Viability Kit (Biolegend); anti-CD4 (cat# 563550 clone SK3, BUV395, 1:25), anti-CD3 (cat# 552851 clone SP34-2, PerCP, 1:20), anti-CD8 (cat# 557945 clone RPA-T8, Alexa Fluor 700, 1:20), anti-CCR7 (cat# 557648 clone 3D12, PE-Cy7, 1:20), anti-CD28 (cat# 563075 clone CD28.2, BV510, 1:20), anti-CD45RA (cat# 562885 clone HI100, BV421, 1:20) (BD Biosciences); anti-CCR2 (cat# 558406 clone 48607, Alexa Fluor 647, 1:5), anti-CCR5 (cat# 556042 PE, 1:5), and anti-CXCR3 (cat# 550967 APC, 1:5) (R&D Systems). Flow cytometric analysis was performed

on BD LSR2 flow cytometer (BD Biosciences); compensation and analysis were performed using Winlist 6.0 (Verity Software House, Inc.).

Chemotaxis assays

Chemotaxis of murine and human effector T cells was assayed in 24 well plates (5 μM pore size transwell insert with polycarbonate membranes; Corning). Media alone (RPMI1640 + 1%BSA) or media containing recombinant chemokines (Peprotech) was placed at the bottom of triplicate wells. Murine T cell migration was assessed at 10 nM murine CXCL10, 1 nM murine CCL2, and 10 nM murine CCL5; human T cell chemotaxis was determined at 100 ng/mL recombinant human or murine chemokine[20] unless otherwise indicated. 5×10^5 cells were fluorescently labeled with CFSE or CTO, placed on the transwell insert, and incubated at 37°C for 3 h. Cells in the bottom chamber were enumerated by flow cytometry using Flow Count Beads (Beckman Coulter). Spontaneous migration was subtracted from all conditions, and data are reported either as absolute number of cells migrated or as migration relative to WT T cells.

In vivo homing assays

Competitive short-term (1 h) homing assays were performed by co-mixing (1:1 ratio) 2.5×10^7 murine $CD8^+$ T cells labeled with 5 - (and 6) - carboxyfluorescein diacetate succinimidyl ester (CFSE) with equal numbers of murine $CD8^+$ T cells labeled with 5 - (and 6) - (4 -chloromethyl) benzoyl) amino) tetramethylrhodamine (CellTracker Orange, Invitrogen Life Technologies) prior to i.v. adoptive transfer. In homing studies using ex vivo activated human T cells, ~1.5×10^7 of CFSE- or CTO-labeled cells were mixed at equivalent numbers prior to injection into tumor-bearing mice. Tumor and spleen were collected 1 h later and mechanically dissociated by Medimachine (BD Biosciences) or passed through a 70 μm nylon cell strainer (BD Biosciences). Ratios of fluorescent adoptively-transferred cells were determined by flow cytometry, and total cell numbers were assessed using Flow Count Beads (Beckman Coulter)[14]. In selected experiments intratumoral infiltration by OT-I cells was monitored using tracking dyes (CellVue Claret, Sigma Aldrich) or by congenic mismatch ($CD45.1^+$ OT-I→$CD45.2^+$ host) up to 3 weeks after transfer.

Quantification of extravasation by transferred $CD8^+$ T cells

After short-term in vivo homing assays, organs were harvested, embedded in optimum cutting temperature compound (OCT, Sakura Finetek) and snap-frozen as previously described[14]. Tissue cryosections (9 μm) were incubated with the primary Ab specific for murine CD31 (cat# 550274 clone MEC 13.3, 20 μg/ml; BD Biosciences) followed by an AMCA fluorochrome-conjugated goat anti-rat secondary Ab (cat# 112-155-003, 1:50; Jackson ImmunoResearch) and imaged using a fluorescence microscope (Olympus Optical) and a SPOT RT camera (Diagnostic Instruments). In experiments in which the location of homed cells was determined (i.e., extravasated vs vessel-associated), all T cells not in contact with $CD31^+$ endothelial cells were designated as extravasated. For consistency, fields containing a minimum of 1 fluorescently-labeled cell were imaged by observers blinded to sample identity, and labeled cells were quantified in ≥ 10 fields (unit area per field, 0.34 mm^2).

Inflammatory monocyte isolation and short-term homing

Tibias and femurs from either WT C57BL/6 or *Ccr2*$^{-/-}$ mice were removed sterilely, and bone marrow was flushed with sterile PBS. RBC were lysed with ACK lysing buffer (Gibco) and inflammatory monocytes were isolated on an AutoMacs machine using positive selection with CD115 microbeads (Miltenyi). WT CD115^{+} cells were labeled with CTO and *Ccr2*$^{-/-}$ CD115^{+} cells were labeled with CFSE, mixed at a 1:1 ratio, and adoptively transferred into B16-OVA-bearing mice. After 2 h, tumor and splenic tissues were analyzed for flow cytometry.

Intravital microscopy

Live imaging of tumor or normal tissues was performed as described[14,27]. Briefly, dorsal skin-flap single-sided window chambers (Research Instruments Inc.) were surgically implanted in C57BL/6 mice and 1 × 10^{5} B16-OVA cells were injected into the center of the chamber. Mice were housed in a 30°C environmental chamber to promote wound-healing and the adhesive qualities of the tumor microvasculature was evaluated ~14–21 days post-implantation. In the indicated studies, T cell interactions were also examined in non-tumor inflamed skin vessels. Following treatment of the mice with STT or LPS, mice were anesthetized (1 mg/ml xylazine and 10 mg/ml ketamine; 10 ml/kg, i.p.) and 5–10 × 10^{7} calcein-labeled effector WT or *Cxcr3*$^{-/-}$ OT-I T cells were injected via tail vein over the 30 min observation period. An epi-illumination intravital microscope with a custom stage equipped with a warming pad and vibration dampening system (Spectra Services) was used to visualize the interactions between the circulating T cells and the microvasculature. Images were captured with an EB charge-coupled device camera (Hamamatsu Photonics) and recorded with a digital videocassette recorder (DSR-11; Sony) and quantified by observers blinded to treatment conditions. T cell interactions were quantified in unbranched vascular segments 100 μm in length with a diameter between 5–40 μm. The rolling fraction was the percentage of total cells that interacted per microvessel; sticking fraction was the percentage of rolling cells that subsequently adhered for ≥30 s[14,27].

In vitro and in vivo cytotoxicity assays

OVA-expressing target cells (either splenocytes pulsed with 5 μg/mL SIINFEKL peptide [InvivoGen], B16-OVA cells, or EG7 cells) were labeled with CFSE and mixed at a 1:1 ratio with CTO-labeled non-antigen-expressing cells (i.e., non-pulsed splenocytes, B16 cells, or EL4 cells, respectively) and incubated in triplicate in the absence of effector T cells, or in the presence of a 15-fold excess of effector WT OT-I or *Cxcr3*$^{-/-}$ OT-I T cells. After 24 h, live cells were analyzed by flow cytometry. For in vivo cytotoxicity assays, OVA-pulsed and non-pulsed splenocytes were mixed at a 1:1 ratio (~4–5 ×10^{6} of each population/mouse) and transferred i.v. into naïve mice in which 3 × 10^{7} WT or *Cxcr3*$^{-/-}$ effector OT-I T cells had been injected 3 h previously. 24 h later, spleens were harvested, lysed, and live cells were analyzed by flow cytometry. The proportion of fluorescently-labeled cells was plotted as CFSE^{+} and CFSE^{-} cells on histograms, and the % specific cytotoxicity was determined by the formula [1-(% CFSE^{-} cells/% CFSE^{+} cells)] × 100%.

Tumor growth studies

WT or *Cxcr3*$^{-/-}$ OT-I effector T cells (5×10^6/mouse) were transferred i.v. into B16-OVA-bearing mice. Experimental endpoints were reached when tumors exceeded 20 mm diameter or mice became moribund. Tumor volumes were calculated by determining the length of short (*l*) and long (*L*) diameters (volume = $l^2 \times L/2$) as described[14].

Statistical analysis

All data shown are the mean ± s.e.m. and group differences were evaluated by unpaired two-tailed Student's *t*-test as described unless otherwise specified. Statistical significance of tumor growth was determined by two-way ANOVA for repeated measures. Survival data were analyzed using Kaplan-Meier log rank tests. P-values < 0.05 were considered significant.

Supplementary Material

Refer to Web version on PubMed Central for supplementary material.

Acknowledgments

We thank K. Curry for technical assistance on transwell assays; S. Kaufman for isolating PBMC from normal human donors; R. Dolnick, K. de Jong, and J. Tario, Jr. for assistance with flow cytometry and Luminex assays; M. Appenheimer for critical reading of the manuscript; and D. Mullins (Geisel School of Medicine at Dartmouth) for guidance on CXCR3-blocking Ab and helpful discussion. This work was supported by the NIH (CA79765 and AI082039 to S.S. Evans; T32 CA085183 and 1F30 CA177210 to M.E. Mikucki; CA069212 to A.D. Luster; CA127475 to T. Gajewski; CA158318-01A1 to K. Odunsi; and the RPCI-UPCI Ovarian Cancer SPORE P50CA159981-01A1 to K. Odunsi and J. Matsuzaki); the Joanna M. Nicolay Foundation to M.E. Mikucki; the University at Buffalo Mark Diamond Research Fund to M.E. Mikucki; the Jennifer Linscott Tietgen Family Foundation to S.S. Evans and J.J. Skitzki; and the Roswell Park/Wilmot Collaborative Grant to S.S. Evans and J. Frelinger.

References

1. Fridman WH, Pages F, Sautes-Fridman C, Galon J. The immune contexture in human tumours: impact on clinical outcome. Nat Rev Cancer. 2012; 12:298–306. [PubMed: 22419253]
2. Sato E, et al. Intraepithelial CD8+ tumor-infiltrating lymphocytes and a high CD8+/regulatory T cell ratio are associated with favorable prognosis in ovarian cancer. Proc Natl Acad Sci U S A. 2005; 102:18538–18543. [PubMed: 16344461]
3. Galon J, et al. Type, density, and location of immune cells within human colorectal tumors predict clinical outcome. Science. 2006; 313:1960–1964. [PubMed: 17008531]
4. Pages F, Galon J, Dieu-Nosjean MC, Tartour E, Sautes-Fridman C, Fridman WH. Immune infiltration in human tumors: a prognostic factor that should not be ignored. Oncogene. 2010; 29:1093–1102. [PubMed: 19946335]
5. Piras F, et al. The predictive value of CD8, CD4, CD68, and human leukocyte antigen-D-related cells in the prognosis of cutaneous malignant melanoma with vertical growth phase. Cancer. 2005; 104:1246–1254. [PubMed: 16078259]
6. Galon J, et al. Cancer classification using the Immunoscore: a worldwide task force. J Transl Med. 2012; 10:205. [PubMed: 23034130]
7. Maus MV, Fraietta JA, Levine BL, Kalos M, Zhao Y, June CH. Adoptive immunotherapy for cancer or viruses. Annu Rev Immunol. 2014; 32:189–225. [PubMed: 24423116]
8. Restifo NP, Dudley ME, Rosenberg SA. Adoptive immunotherapy for cancer: harnessing the T cell response. Nat Rev Immunol. 2012; 12:269–281. [PubMed: 22437939]

9. Muthuswamy R, et al. NF-kappaB hyperactivation in tumor tissues allows tumor-selective reprogramming of the chemokine microenvironment to enhance the recruitment of cytolytic T effector cells. Cancer Res. 2012; 72:3735–3743. [PubMed: 22593190]
10. Topalian SL, et al. Safety, activity, and immune correlates of anti-PD-1 antibody in cancer. N Engl J Med. 2012; 366:2443–2454. [PubMed: 22658127]
11. Hodi FS, et al. Improved survival with ipilimumab in patients with metastatic melanoma. N Engl J Med. 2010; 363:711–723. [PubMed: 20525992]
12. Rosenberg SA, et al. Durable complete responses in heavily pretreated patients with metastatic melanoma using T-cell transfer immunotherapy. Clin Cancer Res. 2011; 17:4550–4557. [PubMed: 21498393]
13. Herbst RS, et al. Predictive correlates of response to the anti-PD-L1 antibody MPDL3280A in cancer patients. Nature. 2014; 515:563–567. [PubMed: 25428504]
14. Fisher DT, et al. IL-6 trans-signaling licenses mouse and human tumor microvascular gateways for trafficking of cytotoxic T cells. J Clin Invest. 2011; 121:3846–3859. [PubMed: 21926464]
15. Gajewski TF, Schreiber H, Fu YX. Innate and adaptive immune cells in the tumor microenvironment. Nat Immunol. 2013; 14:1014–1022. [PubMed: 24048123]
16. Motz GT, et al. Tumor endothelium FasL establishes a selective immune barrier promoting tolerance in tumors. Nat Med. 2014; 20:607–615. [PubMed: 24793239]
17. Kandalaft LE, Facciabene A, Buckanovich RJ, Coukos G. Endothelin B receptor, a new target in cancer immune therapy. Clin Cancer Res. 2009; 15:4521–4528. [PubMed: 19567593]
18. Evans SS, Repasky EA, Fisher DT. Fever and the thermal regulation of immunity: the immune system feels the heat. Nat Rev Immunol. in press. 10.1038/nri3843
19. Griffith JW, Sokol CL, Luster AD. Chemokines and chemokine receptors: positioning cells for host defense and immunity. Annu Rev Immunol. 2014; 32:659–702. [PubMed: 24655300]
20. Harlin H, et al. Chemokine expression in melanoma metastases associated with CD8+ T-cell recruitment. Cancer Res. 2009; 69:3077–3085. [PubMed: 19293190]
21. Mlecnik B, et al. Biomolecular network reconstruction identifies T-cell homing factors associated with survival in colorectal cancer. Gastroenterology. 2010; 138:1429–1440. [PubMed: 19909745]
22. Mullins IM, et al. CXC chemokine receptor 3 expression by activated CD8+ T cells is associated with survival in melanoma patients with stage III disease. Cancer Res. 2004; 64:7697–7701. [PubMed: 15520172]
23. Shulman Z, et al. Transendothelial migration of lymphocytes mediated by intraendothelial vesicle stores rather than by extracellular chemokine depots. Nat Immunol. 2012; 13:67–76. [PubMed: 22138716]
24. Walch JM, et al. Cognate antigen directs CD8+ T cell migration to vascularized transplants. J Clin Invest. 2013; 123:2663–2671. [PubMed: 23676459]
25. Groom JR, et al. CXCR3 chemokine receptor-ligand interactions in the lymph node optimize CD4+ T helper 1 cell differentiation. Immunity. 2012; 37:1091–1103. [PubMed: 23123063]
26. Yokota SJ, et al. Changes in ovarian tumor cell number, tumor vasculature, and T cell function monitored in vivo using a novel xenograft model. Cancer Immun. 2013; 13:11. [PubMed: 23885217]
27. Chen Q, et al. Fever-range thermal stress promotes lymphocyte trafficking across high endothelial venules via an interleukin 6 trans-signaling mechanism. Nat Immunol. 2006; 7:1299–1308. [PubMed: 17086187]
28. Carriere V, et al. Cancer cells regulate lymphocyte recruitment and leukocyte-endothelium interactions in the tumor-draining lymph node. Cancer Res. 2005; 65:11639–11648. [PubMed: 16357175]
29. Seung E, Cho JL, Sparwasser T, Medoff BD, Luster AD. Inhibiting CXCR3-dependent CD8+ T cell trafficking enhances tolerance induction in a mouse model of lung rejection. J Immunol. 2011; 186:6830–6838. [PubMed: 21555535]
30. Khan IA, et al. IP-10 is critical for effector T cell trafficking and host survival in Toxoplasma gondii infection. Immunity. 2000; 12:483–494. [PubMed: 10843381]

31. Mellado M, et al. Chemokine receptor homo- or heterodimerization activates distinct signaling pathways. EMBO J. 2001; 20:2497–2507. [PubMed: 11350939]
32. Contento RL, et al. CXCR4-CCR5: a couple modulating T cell functions. Proc Natl Acad Sci U S A. 2008; 105:10101–10106. [PubMed: 18632580]
33. Qian BZ, et al. CCL2 recruits inflammatory monocytes to facilitate breast-tumour metastasis. Nature. 2011; 475:222–225. [PubMed: 21654748]
34. Budhu S, et al. CD8+ T cell concentration determines their efficiency in killing cognate antigen-expressing syngeneic mammalian cells in vitro and in mouse tissues. J Exp Med. 2010; 207:223–235. [PubMed: 20065066]
35. Castellano M, et al. CDKN2A/p16 is inactivated in most melanoma cell lines. Cancer Res. 1997; 57:4868–4875. [PubMed: 9354451]
36. Wang RF, Robbins PF, Kawakami Y, Kang XQ, Rosenberg SA. Identification of a gene encoding a melanoma tumor antigen recognized by HLA-A31-restricted tumor-infiltrating lymphocytes. J Exp Med. 1995; 181:799–804. [PubMed: 7836932]
37. Bedognetti D, et al. CXCR3/CCR5 pathways in metastatic melanoma patients treated with adoptive therapy and interleukin-2. Br J Cancer. 2013; 109:2412–2423. [PubMed: 24129241]
38. Molon B, et al. Chemokine nitration prevents intratumoral infiltration of antigen-specific T cells. J Exp Med. 2011; 208:1949–1962. [PubMed: 21930770]
39. Hartl D, et al. Infiltrated neutrophils acquire novel chemokine receptor expression and chemokine responsiveness in chronic inflammatory lung diseases. J Immunol. 2008; 181:8053–8067. [PubMed: 19017998]
40. Colvin RA, Campanella GS, Sun J, Luster AD. Intracellular domains of CXCR3 that mediate CXCL9, CXCL10, and CXCL11 function. J Biol Chem. 2004; 279:30219–30227. [PubMed: 15150261]
41. Schumann K, et al. Immobilized chemokine fields and soluble chemokine gradients cooperatively shape migration patterns of dendritic cells. Immunity. 2010; 32:703–713. [PubMed: 20471289]
42. Weber M, et al. Interstitial dendritic cell guidance by haptotactic chemokine gradients. Science. 2013; 339:328–332. [PubMed: 23329049]
43. Shamri R, et al. Lymphocyte arrest requires instantaneous induction of an extended LFA-1 conformation mediated by endothelium-bound chemokines. Nat Immunol. 2005; 6:497–506. [PubMed: 15834409]
44. Mohan K, Cordeiro E, Vaci M, McMaster C, Issekutz TB. CXCR3 is required for migration to dermal inflammation by normal and in vivo activated T cells: differential requirements by CD4 and CD8 memory subsets. Eur J Immunol. 2005; 35:1702–1711. [PubMed: 15884054]
45. Groom JR, Luster AD. CXCR3 ligands: redundant, collaborative and antagonistic functions. Immunol Cell Biol. 2011; 89:207–215. [PubMed: 21221121]
46. Hogg N, Patzak I, Willenbrock F. The insider's guide to leukocyte integrin signalling and function. Nat Rev Immunol. 2011; 11:416–426. [PubMed: 21597477]
47. Basu J, Shin DM, Jo EK. Mycobacterial signaling through toll-like receptors. Front Cell Infect Microbiol. 2012; 2:145. [PubMed: 23189273]
48. Miller SI, Ernst RK, Bader MW. LPS, TLR4 and infectious disease diversity. Nat Rev Microbiol. 2005; 3:36–46. [PubMed: 15608698]
49. Re F, Strominger JL. Toll-like receptor 2 (TLR2) and TLR4 differentially activate human dendritic cells. J Biol Chem. 2001; 276:37692–37699. [PubMed: 11477091]
50. Watari K, Nakaya M, Kurose H. Multiple functions of G protein-coupled receptor kinases. J Mol Signal. 2014; 9:1. [PubMed: 24597858]
51. Reiter E, Lefkowitz RJ. GRKs and beta-arrestins: roles in receptor silencing, trafficking and signaling. Trends Endocrinol Metab. 2006; 17:159–165. [PubMed: 16595179]
52. De Vries L, Zheng B, Fischer T, Elenko E, Farquhar MG. The regulator of G protein signaling family. Annu Rev Pharmacol Toxicol. 2000; 40:235–271. [PubMed: 10836135]
53. Loudon RP, Perussia B, Benovic JL. Differentially regulated expression of the G-protein-coupled receptor kinases, betaARK and GRK6, during myelomonocytic cell development in vitro. Blood. 1996; 88:4547–4557. [PubMed: 8977246]

54. De Blasi A, Parruti G, Sallese M. Regulation of G protein-coupled receptor kinase subtypes in activated T lymphocytes. Selective increase of beta-adrenergic receptor kinase 1 and 2. J Clin Invest. 1995; 95:203–210. [PubMed: 7814617]
55. Vroon A, et al. Reduced GRK2 level in T cells potentiates chemotaxis and signaling in response to CCL4. J Leukoc Biol. 2004; 75:901–909. [PubMed: 14761932]
56. Kleibeuker W, et al. Physiological changes in GRK2 regulate CCL2-induced signaling to ERK1/2 and Akt but not to MEK1/2 and calcium. J Neurochem. 2008; 104:979–992. [PubMed: 17971124]
57. Kveberg L, Ryan JC, Rolstad B, Inngjerdingen M. Expression of regulator of G protein signalling proteins in natural killer cells, and their modulation by Ly49A and Ly49D. Immunology. 2005; 115:358–365. [PubMed: 15946253]
58. Luther SA, Cyster JG. Chemokines as regulators of T cell differentiation. Nat Immunol. 2001; 2:102–107. [PubMed: 11175801]
59. Camargo JF, et al. CCR5 expression levels influence NFAT translocation, IL-2 production, and subsequent signaling events during T lymphocyte activation. J Immunol. 2009; 182:171–182. [PubMed: 19109148]
60. Moon EK, et al. Expression of a functional CCR2 receptor enhances tumor localization and tumor eradication by retargeted human T cells expressing a mesothelin-specific chimeric antibody receptor. Clin Cancer Res. 2011; 17:4719–4730. [PubMed: 21610146]
61. Sharma RK, Chheda Z, Jala VR, Haribabu B. Expression of leukotriene B(4) receptor-1 on CD8(+) T cells is required for their migration into tumors to elicit effective antitumor immunity. J Immunol. 2013; 191:3462–3470. [PubMed: 23960231]
62. Kurachi M, et al. Chemokine receptor CXCR3 facilitates CD8(+) T cell differentiation into short-lived effector cells leading to memory degeneration. J Exp Med. 2011; 208:1605–1620. [PubMed: 21788406]
63. Tran E, et al. Cancer immunotherapy based on mutation-specific CD4+ T cells in a patient with epithelial cancer. Science. 2014; 344:641–645. [PubMed: 24812403]
64. Oghumu S, et al. CXCR3 deficiency enhances tumor progression by promoting macrophage M2 polarization in a murine breast cancer model. Immunology. 2014; 143:109–119. [PubMed: 24679047]
65. von Andrian UH, Mempel TR. Homing and cellular traffic in lymph nodes. Nat Rev Immunol. 2003; 3:867–878. [PubMed: 14668803]
66. Mordelet E, Davies HA, Hillyer P, Romero IA, Male D. Chemokine transport across human vascular endothelial cells. Endothelium. 2007; 14:7–15. [PubMed: 17364892]
67. Hamzah J, et al. Targeted liposomal delivery of TLR9 ligands activates spontaneous antitumor immunity in an autochthonous cancer model. J Immunol. 2009; 183:1091–1098. [PubMed: 19561111]
68. Hong M, et al. Chemotherapy induces intratumoral expression of chemokines in cutaneous melanoma, favoring T-cell infiltration and tumor control. Cancer Res. 2011; 71:6997–7009. [PubMed: 21948969]
69. Arenberg DA, White ES, Burdick MD, Strom SR, Strieter RM. Improved survival in tumor-bearing SCID mice treated with interferon-gamma-inducible protein 10 (IP-10/CXCL10). Cancer Immunol Immunother. 2001; 50:533–538. [PubMed: 11776375]
70. Liu Y, Huang H, Saxena A, Xiang J. Intratumoral coinjection of two adenoviral vectors expressing functional interleukin-18 and inducible protein-10, respectively, synergizes to facilitate regression of established tumors. Cancer Gene Ther. 2002; 9:533–542. [PubMed: 12032664]

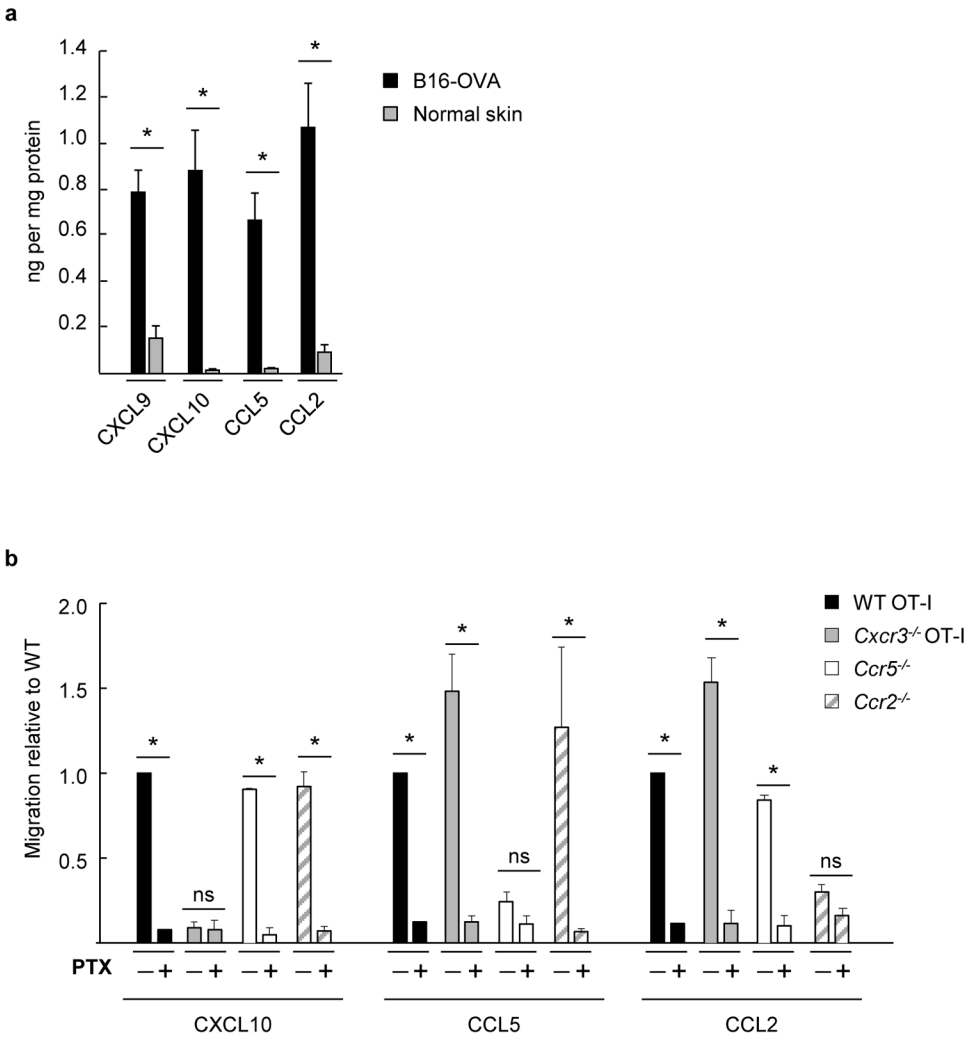

Figure 1. Murine CD8$^+$ effector T cells express an array of functional chemokine receptors complementary for chemokine ligands present in the tumor microenvironment

(**a**) Cognate chemokine ligands for CXCR3, CCR5, and CCR2 (i.e., CXCL9/CXCL10, CCL5, and CCL2, respectively) were quantified by ELISA in B16-OVA tumor extracts (tumor volume ~ 400–500 mm^3) or in normal skin fom tumor-free mice. Data (mean ± s.e.m.) are from ≥3 independent experiments (n ≥2 mice per group). (**b**) Transwell assays were performed where fluorescently-labeled WT OT-I T cells were admixed with equivalent numbers of chemokine receptor-deficient effector cells and tested for migration to the indicated recombinant chemokines. WT and chemokine receptor-deficient cells were also pretreated with the global G-protein inhibitor pertussis toxin (PTX) and migration was quantified by flow cytometry. Background migration (absence of chemokine) was subtracted from all values. Data (mean ± s.e.m.) are represented as migration relative to WT and are from ≥3 independent experiments. (**a, b**) * $P < 0.05$; ns, not significant; unpaired two-tailed Student's *t*-test.

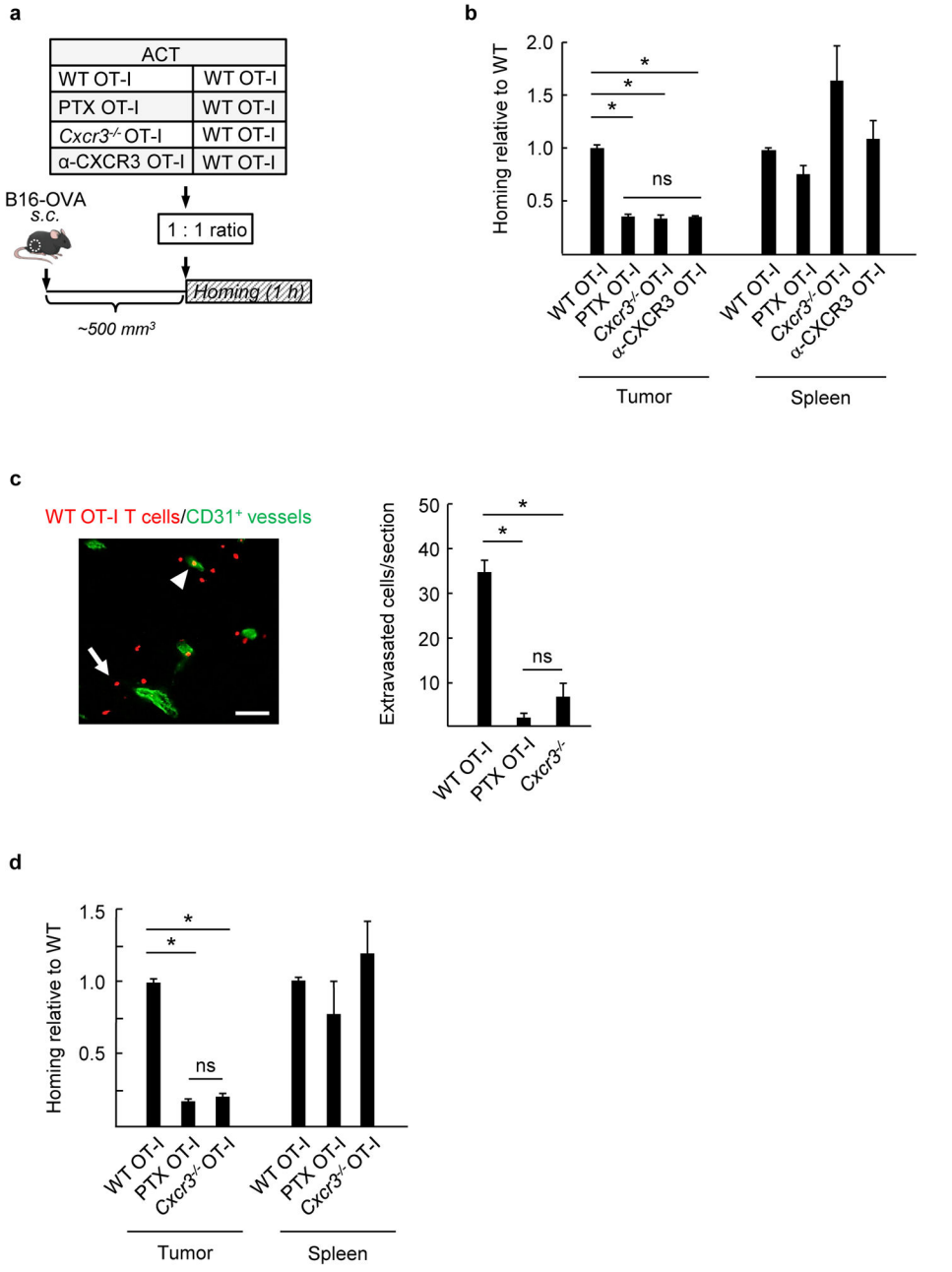

Figure 2. CXCR3 is obligatory for murine CD8$^+$ effector T cell trafficking to melanoma in vivo

(**a**) Experimental scheme for short-term (1 h) competitive homing studies. The groups used for adoptive cell transfer (ACT) included WT OT-I cells comixed at a 1:1 ratio with WT OT-I cells, WT OT-I cells pretreated with PTX, *Cxcr3*$^{-/-}$ OT-I cells, or WT OT-I cells pretreated with α-CXCR3 blocking Ab. Fluorescent-labeled CD8$^+$ effector T cells were injected i.v. into mice with established B16-OVA tumors (tumor volume ~400–500 mm^3) and homing was evaluated after 1 h. (**b**) Data represent ratio of adoptively transferred T cells relative to WT determined by flow cytometry in tumors and spleens following competitive homing assays. (**c**) The number of WT (red) or *Cxcr3*$^{-/-}$ cells which successfully

extravasated into underlying interstitium was quantified in histological tumor sections counterstained with CD31-specific Ab (green) to demark vessels. A representative photomicrograph of homed WT OT-I cells is shown with an example of an extravasated cell indicated by a white arrow and a vessel-associated cell noted by a white arrowhead. Scale bar, 100 μm. (**d**) Ratio of adoptively transferred T cells recovered in B16-OVA tumor-bearing mice pretreated with systemic thermal therapy (STT; 39.5 ± 0.5 °C for 6 h). PTX, pertussis toxin; α-CXCR3, CXCR3 blocking Ab. (**b–d**) All data (mean ± s.e.m.) are from ≥ 3 independent experiments (n ≥ 2 mice per group). ***** $P < 0.001$; ns, not significant; unpaired two-tailed Student's *t*-test.

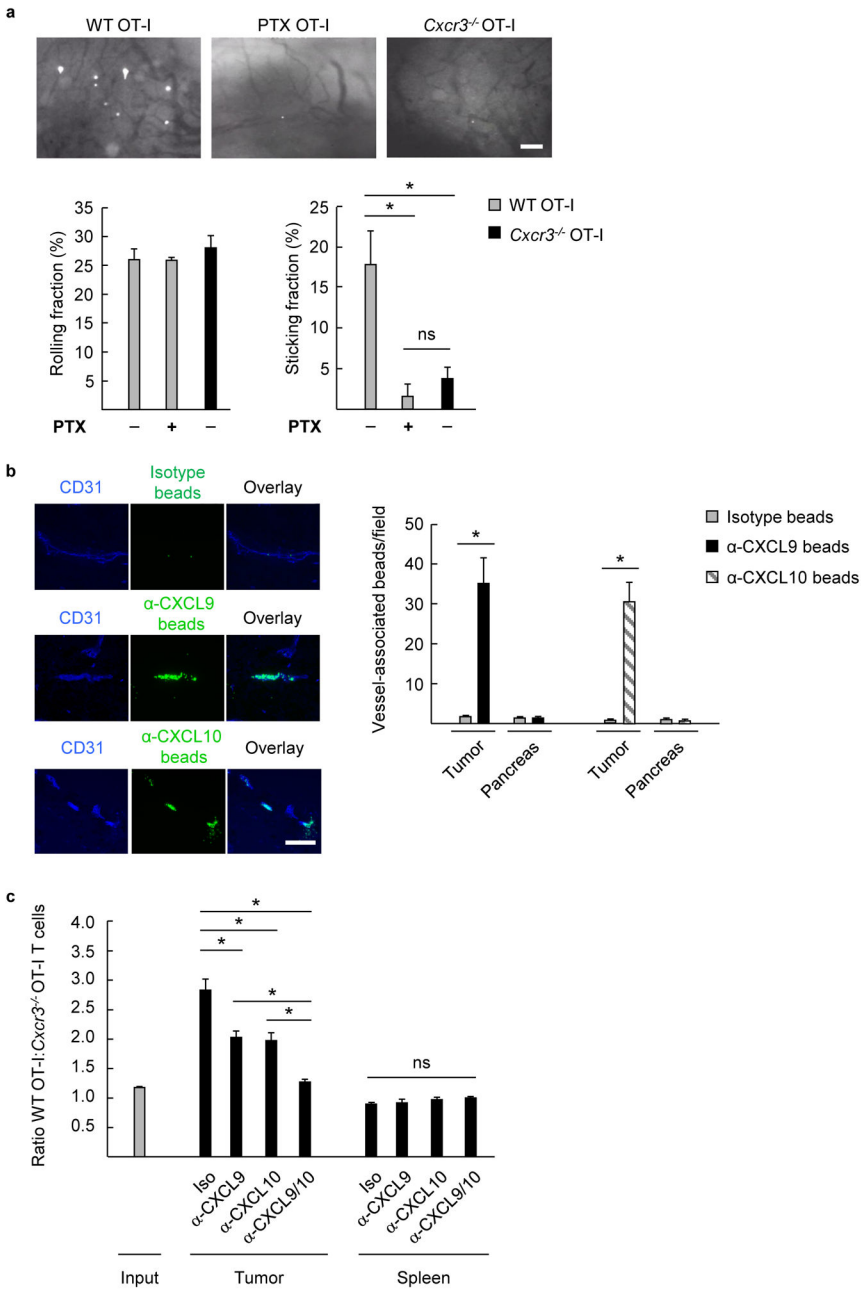

Figure 3. Intravascular CXCR3 ligands support stable adhesion of murine CD8$^+$ T cells within tumor vessels in vivo

(**a**) Representative photomicrographs of intravital microscopy depicting stable interactions of fluorescently-tagged WT OT-I cells, WT OT-I cells pretreated with PTX, or *Cxcr3*$^{-/-}$ OT-I effector cells within B16-OVA tumor vessels in mice pretreated with systemic thermal therapy (STT; core temperature elevated to 39.5 ± 0.5 °C for 6 h). Data (mean ± s.e.m.) for rolling fractions and sticking fractions are from ≥3 independent experiments (n ≥2 mice per group). ***** $P < 0.05$. (**b**) Isotype- and α-CXCL10 or α-CXCL9 Ab-conjugated fluorescent beads (green) were injected into B16-OVA mice by tail vein. Tumor and pancreatic sections were counterstained with anti-CD31 Ab (blue) to identify beads associated with vascular

structures. Representative images from tumors containing isotype, α-CXCL9, or α-CXCL10 Ab-conjugated beads are shown. Data (mean ± s.e.m.) are of 10 fields analyzed from paired mice and are from 3 independent experiments. ***** $P < 0.001$. (**a, b**) Scale bars, 100 μm. (**c**) Mice were treated i.p. with chemokine-neutralizing Ab 3 h prior to competitive homing assays using WT OT-I and *Cxcr3*$^{-/-}$ OT-I effector T cells. The ratio of WT OT-I:*Cxcr3*$^{-/-}$ OT-I cells within tumor and spleen was quantified by flow cytometry. Data (mean ± s.e.m.) are from 3 independent experiments (n = 2 mice per group). ***** $P < 0.04$, compared to isotype or dual Ab treatment. (**a–c**) Data analyzed by unpaired two-tailed Student's *t*-test; ns, not significant.

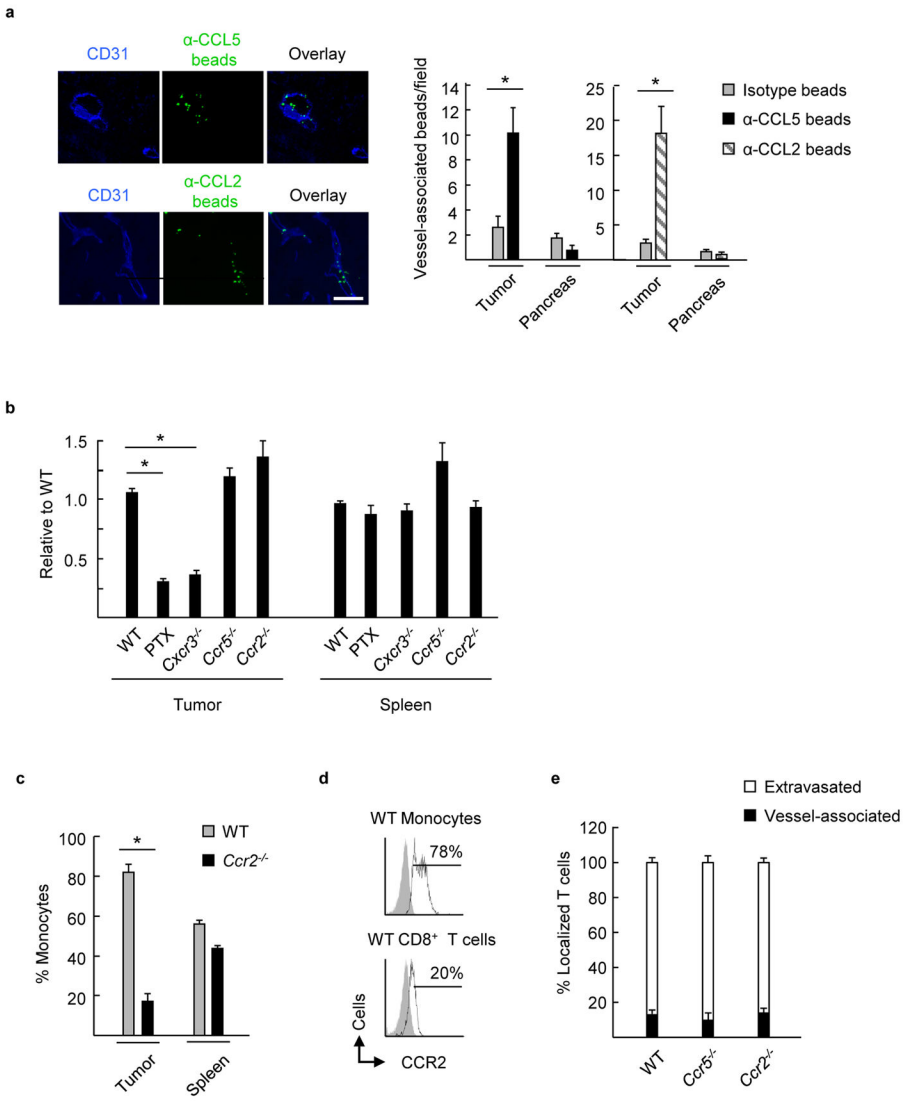

Figure 4. Functional cooperativity of CCR5 and CCR2 is not necessary for CXCR3-dependent trafficking of murine CD8$^+$ effector T cells to tumors

(**a**) Isotype- and α-CCL5 or α-CCL2 Ab-conjugated fluorescent beads (green) were injected into B16-OVA mice by tail vein. Tumor and pancreatic sections were counterstained with anti-CD31 Ab (blue) to identify beads associated with vascular structures. Data (mean ± s.e.m.) are of 10 fields analyzed from paired mice from ≥3 independent experiments. ***** $P <$ 0.003. Scale bar, 100 μm. (**b**) WT effector T cells were comixed at 1:1 ratio with WT cells, WT cells pretreated with PTX, *Cxcr3*$^{-/-}$ cells, *Ccr5*$^{-/-}$ cells, or *Ccr2*$^{-/-}$ cells (all ex vivo activated cells > 88% CD8$^+$; generated from population of pooled spleen/lymph nodes of mice on C57BL/6 background). Ratio of adoptively transferred T cells relative to WT in tumors or spleens of B16-OVA tumor-bearing mice following short-term competitive homing assays is shown. Data (mean ± s.e.m.) are from 3 independent experiments (n ≥ 2 mice per group). ***** $P < 0.001$ compared to WT. (**c**) Percent of adoptively transferred WT and *Ccr2*$^{-/-}$ inflammatory CD115$^+$ monocytes in tumors and spleens of B16-OVA tumor-bearing mice following competitive homing assays. Data (mean ± s.e.m.) are from 3

independent experiments (n = 2 mice per group). * $P < 0.003$ compared to WT. (**d**) Flow cytometric analysis of WT $CD8^+$ effector T cells and inflammatory $CD115^+$ monocytes for surface expression of CCR2 (unfilled histograms); gray-filled histograms represent isotype control Ab staining. (**e**) Histological analysis was performed following short-term competitive homing assays between fluorescently-labeled WT effector $CD8^+$ T cells and *Ccr5*$^{-/-}$, and *Ccr2*$^{-/-}$ effector T cells. The proportion of homed cells which were vessel-associated or extravasated outside $CD31^+$ vessels are shown. Data (mean ± s.e.m.) are from 2 independent experiments (n = 2 mice per group). (**a–c, e**) Data analyzed by unpaired two-tailed Student's *t*-test.

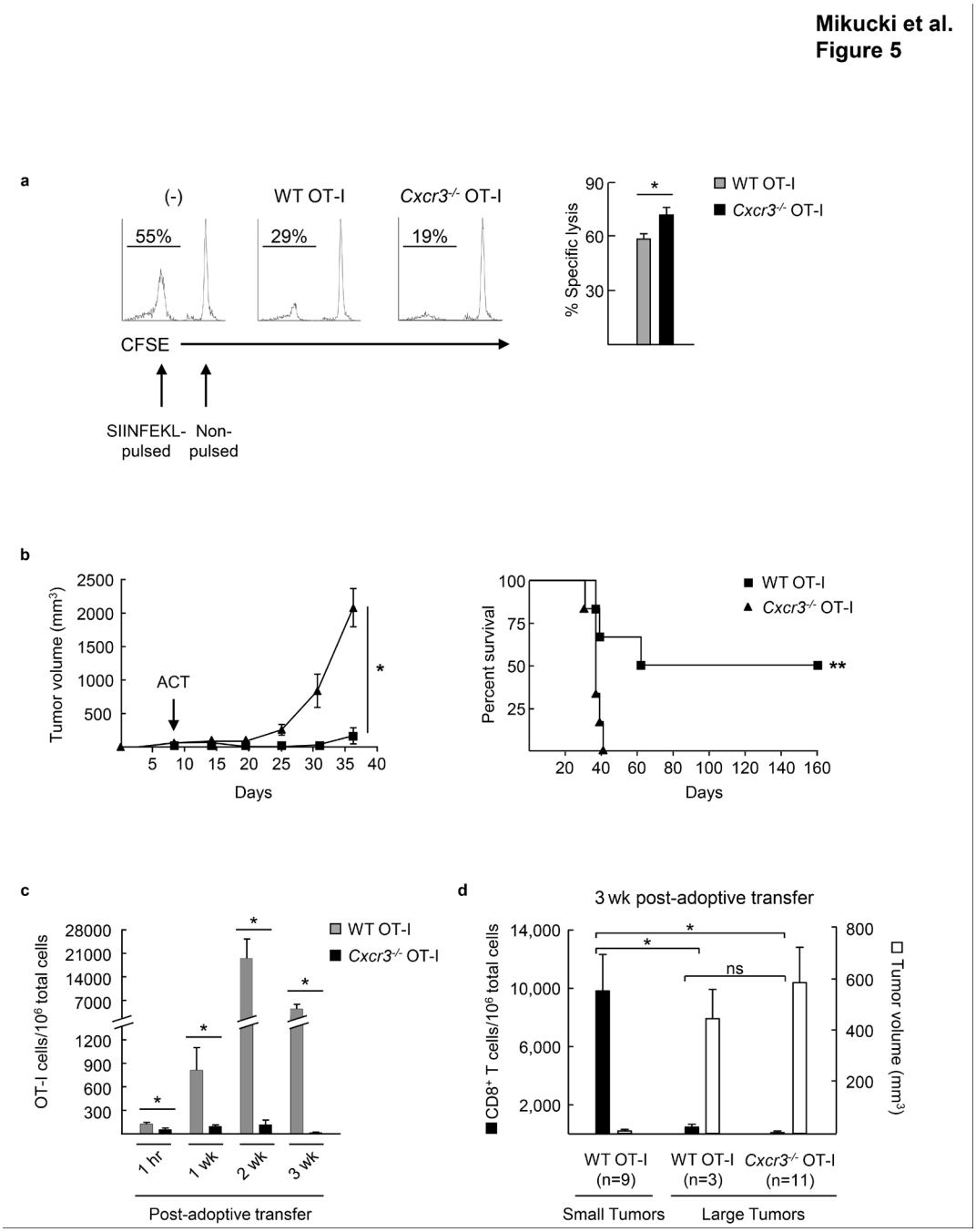

Figure 5. Antitumor efficacy of adoptively transferred CD8$^+$ effector T cells depends on CXCR3 activity

(**a**) In vivo cytotoxicity of SIINFEKL-pulsed splenocytes. WT or *Cxcr3*$^{-/-}$ OT-I effector T cells were transferred into host animals prior to injection of fluorescently-labeled SIINFEKL-pulsed and non-pulsed targets. Spleens were analyzed for target cells by flow cytometry after 24 hrs. Left, representative flow plots of spleens. Right, percent specific lysis of SIINFEKL-pulsed targets. Data (mean ± s.e.m.) are from 2 independent experiments (n = 2 mice per group). * $P < 0.05$. (**b**) WT or *Cxcr3*$^{-/-}$ OT-I effector T cells were

adoptively transferred into mice bearing B16-OVA tumors; time of administration of adoptive cell transfer therapy (ACT) is denoted by the arrow. Tumor growth (left) and survival (right) were monitored over time; complete tumor rejection was detected in 50% of mice treated with WT OT-I cells. Data (mean ± s.e.m.) are representative of 4 independent experiments. ***** $P < 0.001$; ****** $P < 0.02$; statistical significance of tumor growth, two-way ANOVA for repeated measures; survival, Kaplan-Meier log rank tests. (**c, d**) The extent of $CD8^+$ $CD44^+$ OT-I infiltration and (**d**) tumor volume were examined at various times after adoptive transfer using tracking dye; * $P < 0.05$; ns, not significant. (**b–d**) n ≥ 6 mice/group. (**a, c–d**) Data analyzed by unpaired two-tailed Student's *t*-test.

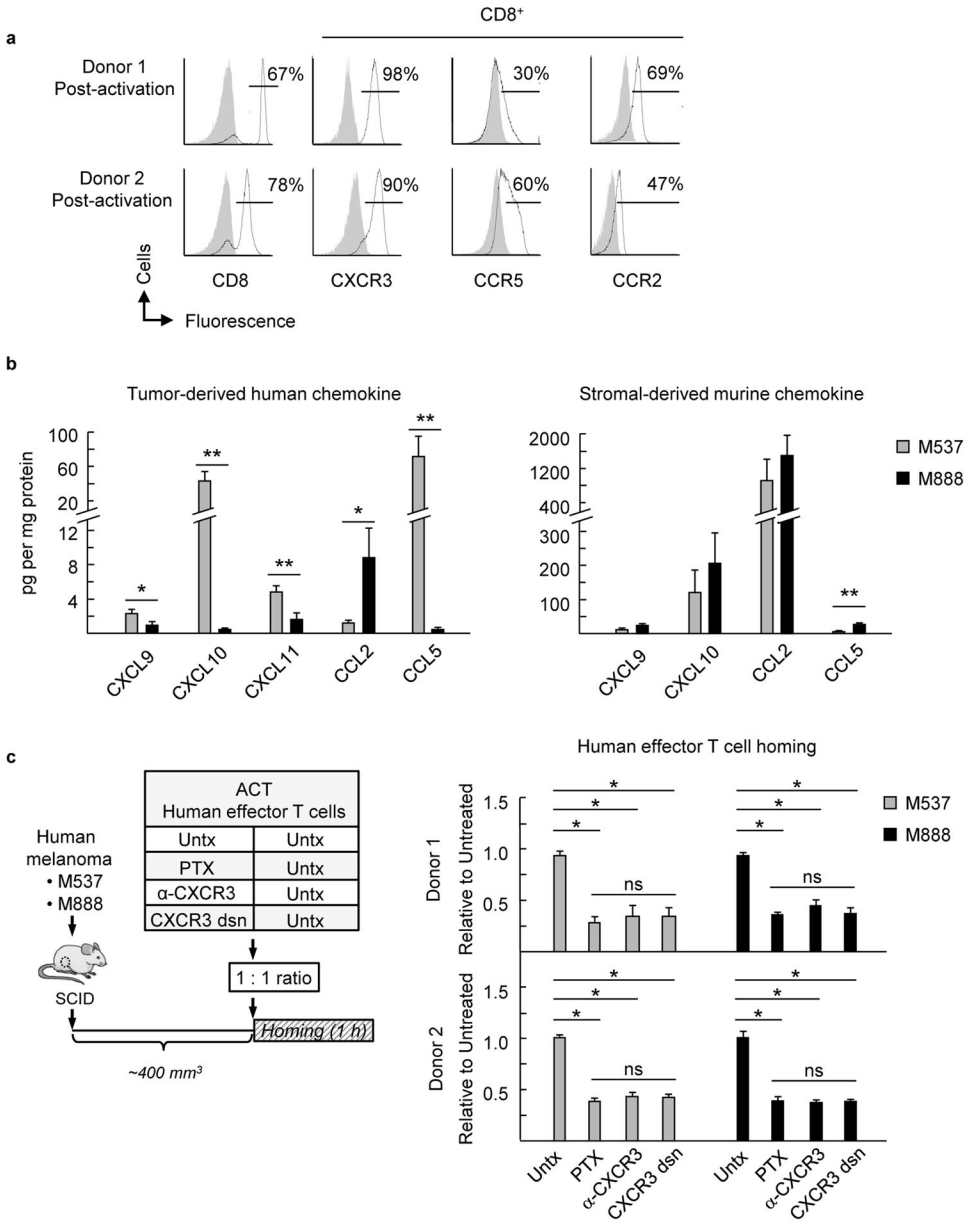

Figure 6. Non-redundant requirement for CXCR3 during human effector T cell trafficking in human melanoma xenografts

(**a**) Chemokine receptor profile on $CD8^+$ T cells (activated ex vivo) from PBL of 2 normal human donors. Gray-filled histograms represent isotype control Ab staining. (**b**) Concentration of human and murine chemokines in tumor extracts from 2 human melanoma xenografts (M537 and M888) was determined by Luminex and ELISA, respectively. Data (mean ± s.e.m.) are from 4 independent experiments (n ≥4 mice per group) for human chemokines and from ≥2 independent experiments (n ≥3 mice per group) for murine chemokines. * $P < 0.05$; ** $P < 0.006$, M537 versus M888 tumors. (**c**) Left, schematic for short-term (1 h) competitive homing studies. The groups used for adoptive cell transfer (ACT) included untreated (Untx) human effector T cells from donor 1 or donor 2 that were

comixed at a 1:1 ratio with untreated cells, PTX-pretreated cells, α-CXCR3 Ab-pretreated cells, or cells where CXCR3 was desensitized by exposure to recombinant CXCL10 prior to transfer into mice (CXCR3 dsn). Right, ratio of adoptively transferred T cells relative to untreated cells in tumors of M537 or M888 tumor-bearing SCID mice following short-term competitive homing assays is shown. PTX, pertussis toxin; α-CXCR3, CXCR3 blocking Ab. Data (mean ± s.e.m.) are from ≥2 independent experiments (n = 2 mice per group). ***** $P <$ 0.02; ns, not significant. (**b–c**) Data analyzed by unpaired two-tailed Student's *t*-test.